14. On RLP2 complexation, the indole NH proton of W118 could not be detected in the NMR spectra obtained in H_2O. This attenuation in intensity is probably not caused by rapid exchange of the NH proton, but instead may be attributed to slow conformational averaging that results in line broadening. The HSQC spectra of both complexes showed that the ^{15}N-^1H correlations of other amide protons at the binding site also have severely attenuated intensities and broadened line widths. In the HSQC spectrum taken with the PLR1-SH3 complex, the ^{15}N-^1H cross-peak of the indole NH of W118 appeared as a weak signal with broadened line width.
15. Structures calculated with the salt bridge restraints are consistent with the experimental data and show good geometry.
16. The D99N mutant was constructed by mutagenesis using polymerase chain reaction according to the megaprimer method [G. Sarker and S. S. Sommer, *BioTechniques* **8**, 404 (1990)]. Procedures for the expression and purification of the mutant were similar to those described for the wild-type SH3 domain (*12*). The D99N mutant protein was correctly folded as shown by a 2D NOESY spectrum.
17. Mutating each of the last two residues of RLP2 to alanine had only a small effect on binding affinity.
18. The significance of a PXXP motif in SH3-ligand recognition was first recognized and brought to our attention by D. Baltimore and colleagues.
19. R. Ren, B. J. Mayer, P. Cicchetti, D. Baltimore, *Science* **259**, 1157 (1993).
20. In both binding orientations, the two critical prolines of the XPpXP motif intercalate into the binding site primarily via the γ and δ methylenes of the proline rings (Fig. 4A), whereas the first and fourth prolines in the PXpPX sequence would interact with the binding site mainly via the β and γ proline methylenes (Fig. 4B). This observation provides an alternative mnemonic device to facilitate the identification of important prolines in an SH3-binding polyproline helix.
21. The affinities of these two PX peptides for D99N SH3 were further decreased, suggesting that the two peptides bind in the expected orientations.
22. SH3-binding sequences from Btk and CDC42 GAP (guanosine triphosphatase activating protein) have lysine at the X_1 site (Table 3).
23. P. Finan *et al.*, *J. Biol. Chem.* **269**, 13752 (1994).
24. M. Rozakis-Adcock, R. Fernley, J. Wade, T. Pawson, D. Bowtell, *Nature* **363**, 83 (1993).
25. R. Kapeller *et al.*, *J. Biol. Chem.* **269**, 1927 (1994); K. Seedorf *et al.*, *ibid.*, p. 16009; S. Tanaka *et al.*, *Proc. Natl. Acad. Sci. U.S.A.* **91**, 3443 (1994); H. Sumimoto *et al.*, *ibid.*, p. 5345; M. Sudol, *Oncogene* **9**, 2145 (1994); G. Cheng, Z.-S. Ye, D. Baltimore, *Proc. Natl. Acad. Sci. U.S.A.* **91**, 8152 (1994); R. Rickles *et al.*, *EMBO J.* **13**, 5598 (1994).
26. C. M. Pleiman, W. M. Hertz, J. C. Cambier, *Science* **263**, 1609 (1994); J. K. Chen and S. L. Schreiber, *Bioorg. Med. Chem. Lett.* **4**, 1755 (1994).
27. A. A. Adzhubei and M. J. E. Sternberg, *J. Mol. Biol.* **229**, 472 (1993).
28. W. A. Lim and F. M. Richards, *Nature Struct. Biol.* **1**, 221 (1994).
29. Sos has an in vitro binding preference for the NH_2-terminal Grb2 SH3 domain [K. Relf, L. Buday, J. Downward, D. A. Cantrell, *J. Biol. Chem.* **269**, 14081 (1994)]. The complementary DNA encoding the NH_2-terminal SH3 domain of Grb2 (residues 1 to 60) was amplified from a human brain stem library, and the polymerase chain reaction product was subcloned into the pGEX-2TK vector (Pharmacia). Expression of the construct in *Escherichia coli* strain BL-21 yielded a glutathione-S-transferase–SH3 fusion protein, which was purified with a glutathione-Sepharose column (Pharmacia LKB) and cleaved with thrombin (Sigma). The cleavage mixture was purified by exclusion chromatography on Sephacryl S-100 (Pharmacia).
30. B. R. Brooks *et al.*, *J. Comput. Chem.* **4**, 187 (1983).
31. A. Nicholls, K. A. Sharp, B. Honig, *Protein Struct. Funct. Genet.* **11**, 281 (1991).
32. We thank C. G. Anklin (Bruker Instruments) and D. C. Dalgarno (ARIAD Pharmaceuticals) for assisting in the acquisition of several NMR data sets. Supported by the National Institute of General Medical Sciences (GM44993). J.K.C. is an NSF predoctoral fellow and the recipient of an American Chemical Society Division of Organic Chemistry graduate student fellowship; J.A.S. is an NIH postdoctoral fellow; S.L.S. is an investigator with the Howard Hughes Medical Institute.

27 July 1994; accepted 5 October 1994

A Central Role of Salicylic Acid in Plant Disease Resistance

Terrence P. Delaney,* Scott Uknes,* Bernard Vernooij, Leslie Friedrich, Kris Weymann, David Negrotto, Thomas Gaffney, Manuela Gut-Rella, Helmut Kessmann, Eric Ward, John Ryals†

Transgenic tobacco and *Arabidopsis thaliana* expressing the bacterial enzyme salicylate hydroxylase cannot accumulate salicylic acid (SA). This defect not only makes the plants unable to induce systemic acquired resistance, but also leads to increased susceptibility to viral, fungal, and bacterial pathogens. The enhanced susceptibility extends even to host-pathogen combinations that would normally result in genetic resistance. Therefore, SA accumulation is essential for expression of multiple modes of plant disease resistance.

Plants have evolved complex, integrated defense mechanisms against disease that include preformed physical and chemical barriers, as well as inducible defenses such as the production of antimicrobial compounds, enhanced strengthening of cell walls, and the production of various antifungal proteins (*1*). Together, these systems form an effective defense against infection, with disease resulting as a rare outcome in the spectrum of plant-microbe interactions. Infectious disease can result when a pathogen is able to overcome the defense processes of a host plant by either actively suppressing or outcompeting them. The ability of a plant to respond to an infection is determined by genetic traits in both the host and pathogen. Many plant resistance (R) genes recognize pathogen molecules resulting from the expression of so-called avirulence (avr) genes (*2*). This interaction often triggers a signal transduction cascade leading to a rapid, host-cell collapse at the site of infection called the hypersensitive reaction (HR) (*3*). Plants also possess an inducible resistance mechanism called systemic acquired resistance (SAR). In experiments with transgenic tobacco plants expressing the bacterial salicylate hydroxylase (*nah*G) gene (NahG plants), we showed that SAR requires the accumulation of SA for its expression (*4*, *5*).

The inability to express SAR in NahG tobacco was also accompanied by larger tobacco mosaic virus (TMV) lesions in these plants than in wild-type (Xanthi) plants (Fig. 1). Eventually, TMV lesions expanded from the leaf to the stem on infected NahG plants. Stem dissection showed that all tissues, including the vascular tissue, had undergone necrosis, which was associated with the presence of viral RNA as determined by RNA hybridization experiments (*6*). Stem necrosis was observed consistently in NahG plants, but not in Xanthi plants. Interestingly, the virus moved virtually unchecked in a cell-to-cell manner, but did not gain access to the phloem and move systemically as it would have in genetically susceptible tobacco plants (*7*).

To determine if increased disease susceptibility was a general feature of NahG plants, we evaluated the development of disease symptoms caused by bacterial and fungal pathogens. NahG plants showed more severe disease symptoms than wild-type plants when inoculated with *Pseudomonas syringae* pv. *tabaci*, *Phytophthora parasitica*, or *Cercospora nicotianae* (Table 1). *Arabidopsis thaliana* ecotype Columbia (Col-0) plants that express the *nah*G gene (*8*) also showed enhanced susceptibility to pathogens. The bacterial pathogen *P. syringae* pv. *tomato* DC3000 (DC3000) is virulent on Col-0 plants and causes symptoms resembling the bacterial speck disease of tomato (*9*). On Col-0 plants, DC3000 caused the formation of small, chlorotic spots on inoculated leaves that were associated with an increase of four to five orders of magnitude in bacterial titer over 5 days (Fig. 2A). However,

T. P. Delaney, S. Uknes, B. Vernooij, L. Friedrich, K. Weymann, D. Negrotto, T. Gaffney, E. Ward, J. Ryals, Agricultural Biotechnology Research Unit, Ciba-Geigy Corporation, P.O. Box 12257, Research Triangle Park, NC, USA.
M. Gut-Rella, Seeds Division, Ciba-Geigy, Ltd., CH-4002 Basel, Switzerland.
H. Kessmann, Plant Protection Division, Ciba-Geigy, Ltd., CH-4002 Basel, Switzerland.

*These authors contributed equally to this study.
†To whom correspondence should be addressed.

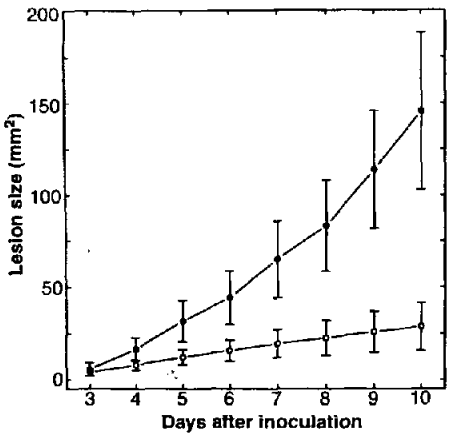

Fig. 1. Tobacco mosaic virus lesion expansion in NahG (closed symbols) and wild-type (open symbols) tobacco. Specific lesion diameters were converted into approximate lesion area (πr^2) for days 3 to 10 after inoculation (mean of at least 112 measurements per data point is plotted with SD).

Table 1. Increased susceptibility of NahG tobacco to bacterial and fungal pathogens. *Pseudomonas syringae* pv. *tabaci* (strain 551, Ciba, Basel, Switzerland) at a concentration of 10^6 colony-forming units (cfu) per milliliter in H_2O was injected into the two lower leaves of several 6- to 7-week-old plants. Six individual plants were evaluated at each time point. Plants infected with *P. syringae* pv. *tabaci* were rated on a five-point disease severity scale, in which 1, 2, 3, 4, and 5 represent 0, 20, 40, 60, 80, and 100%, respectively, of necrotic or chlorotic injected leaf area. *Phytophthora parasitica* was tested and rated as described previously on six individual plants of each type for each time point (*18*). *Cercospora nicotianae* (American Type Culture Collection 18366) spores (1.0×10^5 to 1.5×10^5 spores per milliliter) were sprayed to imminent runoff onto leaf surfaces. The plants were maintained in 100% humidity for 5 days and then misted with water 5 to 10 times per day. The severity of *C. nicotianae* disease was evaluated at each time point by measuring the percentage of infected leaf area on six individual plants. In all cases, mean values are shown followed by the standard deviation. In each of the experiments, a *t* test (least significant difference) was conducted on the evaluations for each day of evaluation; statistically different values between the results obtained for NahG plants and wild-type plants were obtained in the case of each disease.

Disease agent (common name)	Plant genotype	Disease ratings (SD) on days				
		3	4	5		
Pseudomonas syringae pv. *tabaci* (bacterial wildfire)	NahG	2.3 (0.6)	3.3 (0.8)	4.1 (0.7)		
	Wild type	1.5 (0.7)	2.5 (1.1)	2.9 (1.2)		
		6	7	9	11	12
Phytophthora parasitica (black shank)	NahG	2.0 (0.0)	2.5 (0.0)	3.4 (0.2)	4.1 (0.2)	4.7 (0.3)
	Wild type	0.9 (0.5)	1.3 (0.8)	1.9 (1.2)	2.7 (1.1)	3.1 (1.3)
		9	10	12	14	16
Cercospora nicotianae (frog eye leaf spot)	NahG	5.4 (4.5)	15 (6.2)	46 (12.9)	68 (7.7)	97 (4.3)
	Wild type	0.1 (0.5)	2 (1.6)	14 (9.7)	32 (12.0)	81 (19.6)

when *nah*G-expressing plants were inoculated with DC3000, the bacterial titer was 10 to 50 times greater than that seen in nontransgenic controls (Fig. 2A); the increased growth was accompanied by severe disease symptoms (Fig. 2B). *Pseudomonas syringae* pv. *maculicola* strains ES4326 and m4 (*10*) also caused more severe disease symptoms on NahG plants (*6*).

The bacterial avirulence gene *avrRpt2* is recognized by Col-0 plants through a single dominant resistance gene, *Rpt2* (*9*). This pathogen-host combination leads to the reduction of bacterial growth in plants and disease symptoms associated with the HR. After inoculation of Col-0 plants with DC3000 harboring the *avrRpt2* gene, only a 50- to 100-fold increase in bacterial titer was observed (Fig. 2A). In contrast, NahG plants supported the growth of DC3000 (*avrRpt2*) to four to five orders of magnitude (Fig. 2A), which was accompanied by severe disease symptoms (Fig. 2B). Thus, the growth of *avrRpt2*-containing bacteria on NahG plants was similar to that seen on susceptible cultivars of *Arabidopsis*. Suppression of disease resistance by *nah*G in *Arabidopsis* was also seen with *P. syringae* pv. *maculicola* ES4326 containing *avrRpt2* or two other cloned avirulence genes (*avrRpm1* or *avrB*), where resistance is conferred by resistance genes distinct from *Rpt2* (*9–11*).

The Noco race of *Peronospora parasitica* causes downy mildew disease on *Arabidopsis* ecotype Col-0 (Fig. 3A) (*12*). Transgenic Col-0(*nah*G) plants exhibited much greater susceptibility to Noco than wild-type Col-0 did, leading to heavy production of conidia and oospores (Fig. 3B) (*13*). The Wela race of *P. parasitica* is not virulent on Col-0 plants (Fig. 3C), because of a single R gene that triggers a HR upon infection (*12*). However, after infection with Wela, Col-0(*nah*G) plants supported growth of this fungal isolate, resulting in severe disease symptoms and production of abundant hyphae,

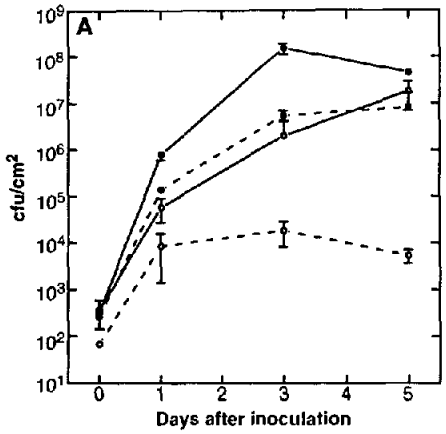

Fig. 2. Increased susceptibility of NahG *Arabidopsis* to *P. syringae* pv. *tomato* DC3000 (DC3000) with and without cloned *avrRpt2*. (**A**) Bacterial growth in NahG (solid symbols) and wild-type (open symbols) plants. Solid lines show DC3000 growth, and dashed lines show growth of DC3000 containing *avrRpt2*. Three samples per time point were harvested after inoculation with 10^5 cfu/ml and the logarithm of the bacterial titer (colony-forming units) per square centimeter of leaf tissue is plotted (mean ± SD). (**B**) Symptoms of plants 5 days after inoculation with DC3000 (left panels) and DC3000 (*avrRpt2*) (right panels). Inoculated leaves (10^5 Cfu/ml) were marked with black ink.

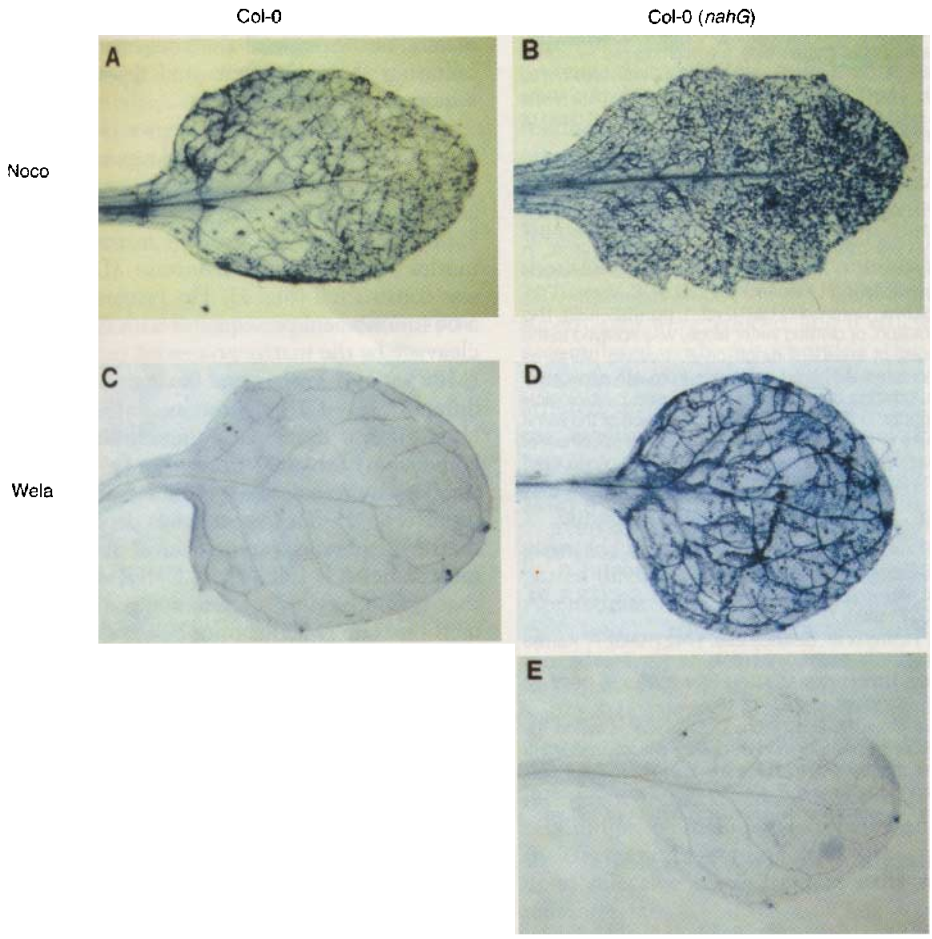

Fig. 3. NahG *Arabidopsis* displays enhanced susceptibility to compatible and incompatible races of *P. parasitica*. (**A** and **B**) Growth of compatible fungal race Noco on wild-type Col-0 (A) and Col-0(*nahG*) (B) plants. (**C** and **D**) Growth of normally incompatible fungal race Wela on wild-type Col-0 (C) and Col-0(*nahG*) (D) plants. INA pretreatment is capable of inducing resistance in Col-0(*nahG*) plants (**E**). Leaves were stained with trypan blue 8 days after inoculation (*13*); leaf vascular tissue is stained pale blue, whereas fungal hyphae and oospores stain more darkly [(A), (B), and (D)].

conidia, and oospores (Fig. 3D). By 3 weeks after inoculation with Wela, NahG plants completely succumbed to the pathogen, which we never see with this *Arabidopsis-Peronospora* interaction. Col-0(*nah*G) plants were also susceptible to another *P. parasitica* race called Emwa (6) to which wild-type Col-0 plants have genetic resistance, encoded by an independent R gene (*12*). These results indicate that expression of *nah*G suppressed the action of R genes that confer resistance to both races of *P. parasitica*.

The synthetic chemical 2,6-dichloroisonicotinic acid (INA) is a functional analog of SA in that treatment of plants with INA induces acquired resistance (*14*, *15*). Treatment of NahG plants with INA before Wela inoculation restored resistance against this pathogen and therefore reversed the effect of the *nah*G gene (Fig. 3E) (*15*). This result demonstrates that the signal transduction mechanism required for genetically determined disease resistance was intact in NahG plants, but failed to function because of the action of salicylate hydroxylase.

After pathogen infection, SAR genes are expressed both at the site of infection and at later times in uninfected tissues (*16*). Because plants that constitutively express SAR genes are resistant to pathogens (*17*, *18*), we asked if susceptibility in NahG plants was associated with reduced SAR gene expression in response to pathogens. After infection with *P. parasitica* race Wela, we analyzed SAR gene expression in Col-0 and NahG plants. *Phytophthora parasitica* infection caused substantial accumulation of *PR-1* mRNA in Col-0 plants, but much less and later in NahG plants (Fig. 4). Similar suppression of gene expression in NahG plants was observed after Noco infection (6). INA pretreatment induced the expression of *PR-1* (Fig. 4), *PR-4*, and *PR-5* (6) in NahG plants and resistance to *P. parasitica* (Fig. 3E). Because INA can induce both SAR gene expression and disease resistance in NahG plants, it is plausible that enhanced disease susceptibility in these plants is due to the disruption of SAR gene expression.

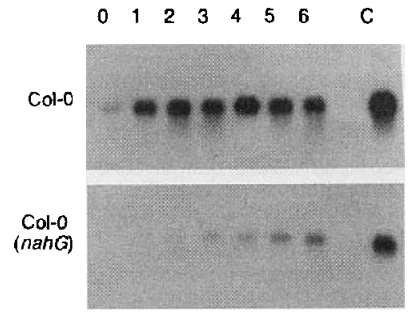

Fig. 4. SAR gene expression in response to pathogen infection. Col-0 and NahG plants were inoculated with the incompatible Wela race of *P. parasitica*. Plants were harvested before and at 1-day intervals after infection. RNA blots were hybridized to an *Arabidopsis PR-1* complementary DNA probe (*14*). Plant genotype and time point (days) are indicated on the left and above the figure, respectively. RNA from INA-treated plants is designated as a control (C).

Expression of the *nah*G gene in plants produces a phenotype of enhanced disease susceptibility and suppression of genetic resistance. We suggest that resistance and susceptibility lie toward the ends of a continuum of host responses to infection. Addition of SA or its functional analog INA can convert a susceptible response into a resistant one. Conversely, substantially decreasing SA concentration can convert interactions that normally result in resistance into susceptible ones. This modulation of the outcome in host-pathogen interactions may be due to either a direct effect of SA itself or to other SA-dependent cellular processes.

Interestingly, similar phenomena have been described in mammalian immune system disorders (*19*). In these cases, a breakdown in signal transduction pathways that modulate disease responses leads to enhanced pathogen susceptibility. Thus, *nah*G-dependent susceptibility in plants shares not only gross phenotypic but also mechanistic analogies with certain immune system defects in mammals. The pleiotropic phenotype of NahG plants suggests that common pathway components participate in multiple modes of disease resistance, including SAR and genetically determined resistance.

REFERENCES AND NOTES

1. C. J. Lamb, M. A. Lawton, M. Dron, R. A. Dixon, *Cell* **56**, 215 (1989); D. Alexander, K. Lawton, S. Uknes, E. Ward, J. Ryals, in *Genetic Engineering: Principles and Methods*, J. K. Setlow, Ed. (Plenum, New York, 1994), vol. 16.
2. N. T. Keen, *Annu. Rev. Genet.* **24**, 447 (1990).
3. E. C. Stakman, *Univ. Minn. Agric. Exp. Sta. Bull.* **138**, 1 (1914); K. O. Müller, in *Plant Pathology: An Advanced Treatise*, J. G. Horsfall and A. E. Dimond, Eds. (Academic Press, New York, 1959), pp. 469–519.
4. T. Gaffney *et al.*, *Science* **261**, 754 (1993).
5. The product of salicylate hydroxylase action on SA is catechol. Applied catechol does not alter TMV lesion

growth. Furthermore, neither SAR gene expression nor resistance is inhibited when SA is co-applied with high concentrations of catechol (B. Vernooij, L. Friedrich, J. Ryals, unpublished results).
6. T. Delaney *et al.*, unpublished results.
7. G. Samuel, *Ann. Appl. Biol.* **21**, 90 (1934); C. Bennett, *J. Agric. Res.* **60**, 361 (1940).
8. *Arabidopsis thaliana* ecotype Col-0 was transformed [H. Huang and H. Ma, *Plant Mol. Biol. Rep.* **10**, 372 (1992)] with *Agrobacterium tumefaciens* strain CIB542 containing the cloned *nahG* gene under the control of an enhanced 35S promoter (*4*). Several independent homozygous transformed lines were identified and with the use of immunoblot analysis were shown to accumulate large amounts of salicylate hydroxylase protein. None of the transformed lines exhibited phenotypes apart from those described.
9. M. C. Whalen, R. W. Innes, A. F. Bent, B. J. Staskawicz, *Plant Cell* **3**, 49 (1991).
10. X. Dong, M. Mindrinos, K. Davis, F. Ausubel, *ibid.*, p. 61; T. Debener, H. Lehnackers, M. Arnold, J. Dangl, *Plant J.* **1**, 289 (1991).
11. B. J. Staskawicz, D. Dahlbeck, N. T. Keen, C. Napoli, *J. Bacteriol.* **169**, 5789 (1987); J. D. Dangl *et al.*, *Plant Cell* **4**, 1359 (1992); R. W. Innes *et al.*, *Plant J.* **4**, 813 (1993); S. R. Bisgrove, M. T. Simonich, N. M. Smith, A. Sattler, R. W. Innes, *Plant Cell* **6**, 927 (1994).
12. E. Koch and A. Slusarenko, *Plant Cell* **2**, 437 (1990); B. Mauch-Mani, K. Croft, A. Slusarenko, in Arabidopsis thaliana *as a Model for Plant-Pathogen Interactions*, K. Davis and R. Hammerschmidt, Eds. (American Phytopathological Society, St. Paul, MN, 1993), pp. 5–20; E. Holub, J. L. Beynon, I. R. Crute, *Mol. Plant-Microbe Interact.* **7**, 223 (1994).
13. Two-week-old *A. thaliana* plants of the indicated ecotype were inoculated with *P. parasitica* (race Wela or Noco) by spraying with a conidia suspension (approximately 1×10^5 spores per milliliter). Inoculated plants were incubated at 17°C under conditions of high humidity. Several plants from each treatment were randomly selected and stained with lactophenol–trypan blue for microscopic examination [R. C. Keogh, B. J. Deverall, S. McLeod, *Trans. Br. Mycol. Soc.* **74**, 329 (1980)]. Trypan blue stains fungal structures within the plant tissue and dead or damaged plant cells.
14. S. Uknes *et al.*, *Plant Cell* **4**, 645 (1992).
15. INA (Ciba-Geigy AG, Basel, Switzerland), formulated as a 25% active ingredient in a wettable powder carrier, was suspended in distilled water at 250 μg of INA per milliliter (325 μM) [J. P. Métraux *et al.*, in *Advances in Molecular Genetics of Plant-Microbe Interactions*, H. Hennecke and D. P. S. Verma, Eds. (Kluwer, Dordrecht, 1991), vol. 1, pp. 432–439]. This solution, or distilled water alone, was sprayed to the point of imminent runoff on *A. thaliana* plants as indicated. Acquired resistance from INA application is indistinguishable from that caused by biological agents, in that both cause the induction of the same suite of SAR genes (*16*) and the same spectrum of pathogen resistance [H. Kessmann *et al.*, *Annu. Rev. Phytopathol.* **32**, 439 (1994)].
16. E. R. Ward *et al.*, *Plant Cell* **3**, 1085 (1991); S. Uknes *et al.*, *Mol. Plant-Microbe Interact.* **6**, 692 (1993).
17. R. A. Dietrich, T. Delaney *et al.*, *Cell* **77**, 565 (1994); K. Broglie *et al.*, *Science* **254**, 1194 (1991).
18. D. Alexander *et al.*, *Proc. Natl. Acad. Sci. U.S.A.* **90**, 7327 (1993).
19. S. Huang *et al.*, *Science* **259**, 1742 (1993); R. Kamijo *et al.*, *ibid.* **263**, 1612 (1994); M. Kondo *et al.*, *ibid.* **262**, 1874 (1993); M. Noguchi *et al.*, *ibid.*, p. 1877; S. M. Russell *et al.*, *ibid.*, p. 1880.
20. We thank M.-D. Chilton, T. Brears, K. Lawton, U. Neuenschwander, and B. Lee for critically reviewing this manuscript. We also thank J. Watkins for preparing media and P. VanBourgondien Jr., S. Sips, and G. Crawford for assistance with plant culture.

26 May 1994; accepted 7 October 1994

The Role of Hsp70 in Conferring Unidirectionality on Protein Translocation into Mitochondria

Christian Ungermann, Walter Neupert,* Douglas M. Cyr

The entry of segments of preproteins of defined lengths into the matrix space of mitochondria was studied. The mitochondrial chaperone Hsp70 (mtHsp70) interacted with proteins emerging from the protein import channel and stabilized translocation intermediates across the membranes in an adenosine triphosphate–dependent fashion. The chaperone bound to the presequence and mature parts of preproteins. In the absence of mtHsp70 binding, preproteins with less than 30 to 40 residues in the matrix diffused out of mitochondria. Thus, protein translocation was reversible up to a late stage. The import channels in both mitochondrial membranes constitute a passive pore that interacts weakly with polypeptide chains entering the matrix.

How proteins are translocated across membranes during the formation of cellular structures is largely unknown (*1*, *2*). Because most proteins are synthesized in the cytosol, proteins destined for subcellular compartments must cross the boundary membranes of organelles. For mitochondria and chloroplasts, proteins must traverse more than one membrane (*3*, *4*). Components of protein translocation machinery and mechanisms for protein targeting have been identified (*1*, *3*), but how protein translocation is driven energetically and rendered unidirectional is still unclear.

In mitochondria, preproteins are transferred from the cytosol into the matrix in several steps (*3*). We investigated events that occur when the NH_2-terminal targeting signal of a mitochondrial precursor protein is translocated across the inner membrane and segments of it emerge in the matrix, and examined the components facilitating these reactions and the energy requirements of this process.

A series of chimeric precursor proteins that consisted of NH_2-terminal regions with various lengths of the *Neurospora crassa* F_o-adenosine triphosphatase (ATPase) subunit 9 precursor (pSu9) (*5*) fused in frame to murine dihydrofolate reductase (DHFR) was constructed (Fig. 1). The precursor has a 66–amino acid presequence with sites for cleavage by the matrix processing peptidase (MPP) at positions 35 and 66. Import of the different Su9-DHFR proteins into mitochondria was measured by monitoring the conversion of the larger precursor (p) to the smaller intermediate (i) and mature (m) forms (Fig. 1). This process was dependent on the membrane potential across the inner membrane, $\Delta\Psi$ (Fig. 1). A DHFR domain that is stabilized by a folate antagonist like methotrexate (Mtx) cannot be translocated across the mitochondrial membranes (*6*, *7*). In the absence of Mtx, the Su9-DHFR fusion proteins were completely imported into the matrix and processed by MPP to the m form (Fig. 1). Import of such fusion proteins into mitochondria in the presence of Mtx led to the formation of translocation intermediates that spanned both membranes, with the folded DHFR domain remaining on the mitochondrial surface. In the presence of Mtx, pSu9(1–86)-DHFR was imported and accumulated predominantly in the p form. A small quantity of the i form was observed after 10 min, and additional processing was seen after longer incubation periods (*8*). The first cleavage site on pSu9(1–86)-DHFR was not readily accessible to MPP in the matrix; and pSu9(1–94)-DHFR was processed to the i form more efficiently. This is in agreement with the observation that approximately 50 amino acid residues are required to span both outer and inner membranes (*7*). In the presence of Mtx, pSu9(1–112)-DHFR also entered the matrix far enough to allow processing from the p to the i form (Fig. 1) (*9*).

The i form of Su9(1–94)-DHFR did not accumulate in large amounts over time when import was arrested with Mtx (Fig. 1). Most of the iSu9(1–94)-DHFR formed was recovered in the supernatant of the import reaction (Fig. 1) (*9*). Its appearance in the supernatant was dependent on $\Delta\Psi$, time, and the addition of Mtx to reaction mixtures. In contrast, pSu9(1–86)-DHFR and iSu9(1–112)-DHFR were found primarily in association with mitochondria in the presence of Mtx (Fig. 1). Experiments with mitochondria from *N. crassa* yielded similar results (*8*).

When the DHFR domain on pSu9(1–94)-DHFR was stabilized by Mtx, the NH_2-terminus of this precursor was translocated

Institut für Physiologische Chemie der Universität München, Goethestr. 33, D-80336 München, Germany.

*To whom correspondence should be addressed.